 CMES, vol.13, no.3, pp.171-183, 2006

A comparison study on different MLPG(LBIE) formulations

V. Vavourakis[1], E. J. Sellountos[2] and D. Polyzos[3]

Abstract: Comparison studies on the accuracy provided by five different elastostatic Meshless Local Petrov-Galerkin (MLPG) type formulations, based on Local Boundary Integral Equation (LBIE) considerations, are made. The main differences of these MLPG(LBIE) formulations, as they compared to each other, are concentrated on the treatment of tractions on the local and global boundaries and the way of imposing the boundary conditions of the elastostatic problem. Both the Moving Least Square (MLS) approximation scheme and the Radial Basis Point Interpolation Functions (RBPIF) are exploited for the interpolation of the interior and boundary variables. Two representative elastostatic problems are solved and the relative error L_2 norms of displacements obtained by the aforementioned MLPG(LBIE)/MLS and MLPG(LBIE)/RBPIF formulations are evaluated for regular and irregular distributions of nodal points, as well as for different support domain radii. Useful conclusions on the accuracy and the stability of a MLPG(LBIE) method are addressed.

keyword: Meshless Local Petrov-Galerkin method, MLPG, Local Boundary Integral Equation method, LBIE, MLS, RBPIF, elasticity.

1 Introduction

Eight years ago, [Zhu, Zhang, and Atluri (1998a)] proposed a meshless Local Boundary Integral Equation (LBIE) method, which gained considerable attention since it seems to circumvent some well-known drawbacks related to a conventional boundary element formulation [Beskos (1987, 1997); Polyzos, Tsinopoulos, and Beskos (1998)] offering simultaneously the advantages of a meshless method where neither domain nor surface discretization is required. In this LBIE methodology, properly distributed nodal points without connectivity requirements, covering the domain of interest as well as the surrounding global boundary are employed instead of any boundary or finite element discretization. All nodal points belong in regular sub-domains (e.g. circles for two-dimensional problems) centered at the corresponding collocation points. At each nodal point, the field is represented through the conventional integral equation used in a Boundary Element Method (BEM) containing, however, integrals defined on the regular boundary of the aforementioned subdomains. The field at the local and global boundaries as well as in the interior of the sub-domains are approximated by a Moving Least Square (MLS) scheme. Owing to regular shapes of the sub-domains, both surface and volume integrals are easily evaluated. The local nature of the sub-domains leads to a final linear system of equations the coefficient matrix of which is sparse and not fully-populated as in the case of the BEM.

At the same time with the LBIE method, [Atluri and Zhu (1998)] proposed a new meshless method, called Meshless Local Petrov-Galerkin (MLPG) method, as an alternative to the Finite Element Method. Depending on the test functions used in the weak formulation of the MLPG method, Atluri and co-workers developed six different MLPG methodologies numbered from one to six [Atluri and Shen (2002a,b)]. The MLPG4 method utilizes as test functions, the fundamental solution of the differential equation (or part of the differential equation) of the problem, resulting thus to a MLPG approach that is equivalent to the LBIE method. Adopting this nomenclature, the initials MLPG(LBIE) instead of LBIE are used in the present work.

After the pioneering work of [Zhu, Zhang, and Atluri (1998a)], several papers on the MLPG(LBIE) method have been appeared in the literature. The most representative are those of [Zhu, Zhang, and Atluri (1998a,b, 1999); Qian, Han, and Atluri (2004)], for linear and

[1] Dept. of Mech. Engineering and Aeronautics; University of Patras (Greece), Institute of Chem. Engng. and High Temperature Process ICETH-FORTH (Rio Greece)
[2] Dept. of Mech. Engineering and Aeronautics; University of Patras (Greece)
[3] Dept. of Mech. Engineering and Aeronautics; University of Patras (Greece), Institute of Chem. Engng. and High Temperature Process ICETH-FORTH (Rio Greece)

non linear acoustic and potential problems, the works of [Sladek, Sladek, and Keer (2000); Atluri, Sladek, Sladek, and Zhu (2000); Atluri and Zhu (2000); Sladek, Sladek, and Keer (2000); Atluri, Han, and Shen (2003); Han and Atluri (2004)] dealing with non-homogeneous and linear elastic problems, the papers of [Sladek, Sladek, and Zhang (2005a,b)] for functionally graded elastic materials, the works of [Long and Zhang (2002); Sladek, Sladek, and Mang (2002a,b); Sladek and Sladek (2003)] for plates, the papers of [Sladek, Sladek, and Atluri (2001); Sladek, Sladek, Krivacek, and Zhang (2003)] concerning thermoelastic and transient heat conduction problems, respectively and the works of [Sladek and Sladek (2003); Sladek, Sladek, and Bazant (2003)] for micropolar and non-local elastic problems. Details concerning the numerical implementation of a MLPG(LBIE) method, integration techniques and the representation of field variables through meshless interpolation schemes can be found in the works of [Atluri, Kim, and Cho (1999); Atluri and Zhu (2000); Sladek, Sladek, and Keer (2000)]. Finally, a comprehensive presentation on the application of the MLPG(LBIE) method to different types of boundary value problems one can find in the review paper of [Sladek, Sladek, and Atluri (2002)] and in the book of [Atluri (2004)].

Very recently, [Sellountos and Polyzos (2003, 2005a,b)] proposed a new MLPG(LBIE) method for solving static, harmonic and transient linear elastic problems. The main advantage of this method, as it is compared to the corresponding ones proposed by Atluri, Sladek brothers and co-workers, is the treatment of boundary tractions as independent variables avoiding thus the use of derivatives of the shape functions involved in the MLS approximation scheme. Although very accurate, its requirement for using uniform distribution of nodal points throughout the analyzed domain confines the robustness of the method. In order to avoid this drawback, [Sellountos, Vavourakis, and Polyzos (2005)] proposed a new version of the above MLPG(LBIE) method, where for the nodal points lying on the global boundary both the displacement and the corresponding traction local boundary integral equations are employed. Thus, for any distribution of points, the advantage of treating displacements and tractions as independent variables remains.

The main goal of the present work is first to investigate the influence of the derivatives of both the Moving Least Square (MLS) shape functions and the Radial Basis Point Interpolation Functions (RBPIF) on the accuracy of a MLPG(LBIE) formulation and second to examine the MLPG(LBIE) solution accuracy in terms of displacements for uniformly distributed and irregular nodal points. To this end, the displacement relative error L_2 norms of five different elastostatic MLPG(LBIE) formulations are compared for uniform and non-uniform distribution of nodal points. Their differences, as they compared to each other, are the treatment of tractions on the local and global boundaries and the way of imposing the boundary conditions of the elastostatic problem. Both the MLS and RBPIF collocation schemes are exploited for the interpolation of the interior and boundary variables and presented in brief in the next section. The aforementioned five MLPG(LBIE) formulations are presented in section three. Two representative elastostatic problems are solved in section four and the displacement relative error L_2 norms provided by the five MLPG(LBIE)/MLS and MLPG(LBIE)/RBPIF formulations are evaluated for different support domain radii.

2 Approximation and Interpolation schemes

In this section the MLS approximation and the RBPIF used for the approximation and the interpolation, respectively, of the considered fields at any point of domain of interest, are presented in brief.

Consider a domain Ω surrounded by a boundary Γ, both covered by arbitrary distributed points $\mathbf{x}^{(k)}$, as shown in Fig. 1. Each point belongs to the interior of a small domain $\Omega_{(k)}$, called support domain. In the present work the support domains of all nodes are considered to be circles with center $\mathbf{x}^{(k)}$ and radius $r_0^{(k)}$, as it is depicted in Fig. 1. For an arbitrary point $\mathbf{y}$, the support subdomains $\Omega_{(j)}$ of the adjacent nodal points $\mathbf{x}^{(j)}$, $j = 1, \ldots, n$ that contain $\mathbf{y}$ define a non-circular subdomain: $\hat{\Omega}_{\mathbf{y}} = \Omega_{(1)} \cup \cdots \cup \Omega_{(n)}$, called domain of definition of $\mathbf{y}$.

2.1 Moving Least Squares approximation

The MLS scheme approximates the displacement field at a point $\mathbf{y}$ of an elastic body according to the following expression [Lancaster and Salkauskas (1981)]

$$u_i(\mathbf{y}) = \mathbf{p}(\mathbf{y}) \cdot \mathbf{a}^{(i)}(\mathbf{y}) \tag{1}$$

where $\mathbf{a}^{(i)}$ is a vector of unknown coefficients and $\mathbf{p}$ is a vector the components of which form a complete basis of

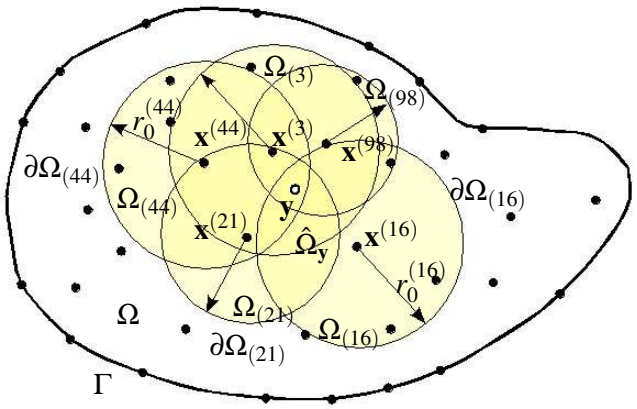

Figure 1 : The circular support domains $\Omega_{(j)}$ and the non-circular domain of definition $\hat{\Omega}_{\mathbf{y}}$ used for the approximation of the field at point $\mathbf{y}$.

monomials of the spatial variables y_i. A quadratic basis is adopted herein, i.e.

$$\mathbf{p}(\mathbf{y}) = \left\{1 \quad y_1 \quad y_2 \quad y_1^2 \quad y_1 y_2 \quad y_2^2\right\} \tag{2}$$

The m unknown coefficients of $\mathbf{a}^{(i)}$ are determined by minimizing the L_2-norm:

$$J_i = \sum_{j=1}^{n} w\left(\mathbf{y},\mathbf{x}^{(j)}\right)\left[\mathbf{p}\left(\mathbf{x}^{(j)}\right)\cdot\mathbf{a}^{(i)}(\mathbf{y}) - \hat{u}_i\left(\mathbf{x}^{(j)}\right)\right]^2 \tag{3}$$

where $\hat{u}_i\left(\mathbf{x}^{(j)}\right)$ is the unknown fictitious nodal displacement at node $\mathbf{x}^{(j)}$ and $w\left(\mathbf{y},\mathbf{x}^{(j)}\right)$ stands for a weighted function, which for the present work is chosen to be the Gaussian weighted one written as

$$w\left(\mathbf{y},\mathbf{x}^{(j)}\right) = 1.0 + \frac{e^{-(d_j/c)^{2k}} - 1.0}{1.0 - e^{-(r_0^{(j)}/c)^{2k}}} \tag{4}$$

with the constants: $k = 1$ and $c = 4.2$, d_j being the Euclidean distance between the evaluation point $\mathbf{y}$ and the point $\mathbf{x}^{(j)}$ the support domain of which is defined by the radius $r_0^{(j)}$.

The minimization of J_i leads to the linear relation:

$$\tilde{\mathbf{A}}\left(\mathbf{y},\mathbf{x}^{(j)}\right)\cdot\mathbf{a}^{(i)}(\mathbf{y}) = \tilde{\mathbf{B}}\left(\mathbf{y},\mathbf{x}^{(j)}\right)\cdot\hat{\mathbf{u}}^{(i)} \tag{5}$$

where

$$\hat{\mathbf{u}}^{(i)} = \left\{\hat{u}_i\left(\mathbf{x}^{(1)}\right) \quad \ldots \quad \hat{u}_i\left(\mathbf{x}^{(n)}\right)\right\}^T \tag{6}$$

$$\tilde{\mathbf{A}}\left(\mathbf{y},\mathbf{x}^{(j)}\right) = \sum_{i=1}^{n} w\left(\mathbf{y},\mathbf{x}^{(i)}\right)\mathbf{p}\left(\mathbf{x}^{(i)}\right)\otimes\mathbf{p}\left(\mathbf{x}^{(i)}\right) \tag{7}$$

$$\tilde{\mathbf{B}}\left(\mathbf{y},\mathbf{x}^{(j)}\right) = \begin{bmatrix} w\left(\mathbf{y},\mathbf{x}^{(1)}\right)\mathbf{p}\left(\mathbf{x}^{(1)}\right) \\ \vdots \\ w\left(\mathbf{y},\mathbf{x}^{(n)}\right)\mathbf{p}\left(\mathbf{x}^{(n)}\right) \end{bmatrix}^T \tag{8}$$

If matrix $\tilde{\mathbf{A}}$ is non-singular and $n \geq m$ then

$$\mathbf{a}^{(i)}(\mathbf{y}) = \tilde{\mathbf{A}}^{-1}\left(\mathbf{y},\mathbf{x}^{(j)}\right)\cdot\tilde{\mathbf{B}}\left(\mathbf{y},\mathbf{x}^{(j)}\right)\cdot\hat{\mathbf{u}}^{(i)} \tag{9}$$

Inserting Eq. 9 into Eq. 1 the following MLS displacement scheme is obtained

$$u_i(\mathbf{y}) = \mathbf{p}(\mathbf{y})\cdot\tilde{\mathbf{A}}^{-1}\left(\mathbf{y},\mathbf{x}^{(j)}\right)\cdot\tilde{\mathbf{B}}\left(\mathbf{y},\mathbf{x}^{(j)}\right)\cdot\hat{\mathbf{u}}^{(i)} \tag{10}$$

written in vector form as

$$\mathbf{u}(\mathbf{y}) = \sum_{j=1}^{n}\phi\left(\mathbf{y},\mathbf{x}^{(j)}\right)\hat{\mathbf{u}}\left(\mathbf{x}^{(j)}\right) \tag{11}$$

with $\hat{\mathbf{u}}\left(\mathbf{x}^{(j)}\right)$ being the unknown fictitious vector field at node $\mathbf{x}^{(j)}$ and

$$\phi\left(\mathbf{y},\mathbf{x}^{(j)}\right) = \sum_{i=1}^{m} p_i\left(\mathbf{x}^{(j)}\right)\left[\tilde{\mathbf{A}}^{-1}\left(\mathbf{y},\mathbf{x}^{(j)}\right)\cdot\tilde{\mathbf{B}}\left(\mathbf{y},\mathbf{x}^{(j)}\right)\right]_{ij} \tag{12}$$

the so called MLS shape functions.

The approximation of the traction vector $\mathbf{t}(\mathbf{y})$ defined at a boundary point $\mathbf{y}$ can be accomplished either by writing it as a combination of the adjacent nodal fictitious displacement vectors $\hat{\mathbf{u}}\left(\mathbf{x}^{(j)}\right)$ or by considering the boundary nodal traction vector as independent variable of the problem. In the first case tractions are expressed through displacements $\hat{\mathbf{u}}$ by substituting the MLS approximation Eq. 11 into the definition of tractions. Specifically, applying the gradient operator on Eq. 11 yields

$$\nabla_{\mathbf{y}}\mathbf{u}(\mathbf{y}) = \sum_{j=1}^{n}\nabla_{\mathbf{y}}\phi\left(\mathbf{y},\mathbf{x}^{(j)}\right)\otimes\hat{\mathbf{u}}\left(\mathbf{x}^{(j)}\right) \tag{13}$$

where the components of the vector $\nabla_{\mathbf{y}}\phi\ (\equiv\phi_{,y})$ are given by

$$\begin{aligned}\phi_{,y}\left(\mathbf{y},\mathbf{x}^{(j)}\right) = \sum_{i=1}^{m}\Big\{ & p_i\left(\mathbf{x}^{(j)}\right)\left[\tilde{\mathbf{A}}^{-1}\left(\mathbf{y},\mathbf{x}^{(j)}\right)\cdot\tilde{\mathbf{B}}_{,y}\left(\mathbf{y},\mathbf{x}^{(j)}\right)\right. \\ & \left. + \tilde{\mathbf{A}}_{,y}^{-1}\left(\mathbf{y},\mathbf{x}^{(j)}\right)\cdot\tilde{\mathbf{B}}\left(\mathbf{y},\mathbf{x}^{(j)}\right)\right]_{ij} \\ & + p_{i,y}\left(\mathbf{x}^{(j)}\right)\left[\tilde{\mathbf{A}}^{-1}\left(\mathbf{y},\mathbf{x}^{(j)}\right)\cdot\tilde{\mathbf{B}}\left(\mathbf{y},\mathbf{x}^{(j)}\right)\right]_{ij}\Big\}\end{aligned} \tag{14}$$

Applying Hooke's law on Eq. 11 and taking into account Eq. 13 and Eq. 14, the MLS approximation of a traction vector at $\mathbf{y}$ is finally written in the form [Sladek, Sladek, and Mang (2002a)]

$$\mathbf{t}(\mathbf{y}) = \tilde{\mathbf{N}}(\mathbf{y}) \cdot \tilde{\mathbf{D}} \cdot \sum_{j=1}^{n} \tilde{\mathbf{E}}\left(\mathbf{y}, \mathbf{x}^{(j)}\right) \cdot \hat{\mathbf{u}}\left(\mathbf{x}^{(j)}\right) \tag{15}$$

where

$$\tilde{\mathbf{D}} = \begin{bmatrix} \lambda+2\mu & \lambda & 0 \\ \lambda & \lambda+2\mu & 0 \\ 0 & 0 & \mu \end{bmatrix} \tag{16}$$

$$\tilde{\mathbf{N}}(\mathbf{y}) = \begin{bmatrix} \hat{n}_1 & 0 & \hat{n}_2 \\ 0 & \hat{n}_2 & \hat{n}_1 \end{bmatrix} \tag{17}$$

$$\tilde{\mathbf{E}}\left(\mathbf{y}, \mathbf{x}^{(j)}\right) = \begin{bmatrix} \phi_{,1}\left(\mathbf{y}, \mathbf{x}^{(j)}\right) & 0 \\ 0 & \phi_{,2}\left(\mathbf{y}, \mathbf{x}^{(j)}\right) \\ \phi_{,2}\left(\mathbf{y}, \mathbf{x}^{(j)}\right) & \phi_{,1}\left(\mathbf{y}, \mathbf{x}^{(j)}\right) \end{bmatrix} \tag{18}$$

with λ, μ being the Lamé constants and $\hat{n}_i$ the unit normal vector component at $\mathbf{y}$.

In the second case where the boundary tractions are considered as independent variables of the problem, the MLS approximation of $\mathbf{t}$ can be accomplished directly through the relation

$$\mathbf{t}(\mathbf{y}) = \sum_{j=1}^{n} \phi\left(\mathbf{y}, \mathbf{x}^{(j)}\right) \hat{\mathbf{t}}\left(\mathbf{x}^{(j)}\right) \tag{19}$$

where the fictitious nodal tractions $\hat{\mathbf{t}}$ are zero for internal nodes and unknown vectors for the nodes lying on the global boundary Γ. In other words, the approximation Eq. 19 utilizes all the nodal points belonging in the domain of definition $\hat{\Omega}_{\mathbf{y}}$ in order to define the shape functions, employs however, only the traction vectors of the adjacent boundary nodes to approximate the traction vector at $\mathbf{y}$.

2.2 Radial Basis Point Interpolation Functions

The RBPIF scheme interpolates the displacement field at a point $\mathbf{y}$ of an elastic body using both a polynomial basis function $\mathbf{p}$ and a radial basis function $\mathbf{b}$, as follows [Wendland (1999); Wang and Liu (2002)]

$$u_i(\mathbf{y}) = \mathbf{p}(\mathbf{y}) \cdot \mathbf{a}^{(i)}(\mathbf{y}) + \mathbf{b}(\mathbf{y}) \cdot \mathbf{c}^{(i)}(\mathbf{y}) \tag{20}$$

where $\mathbf{a}^{(i)}$ and $\mathbf{c}^{(i)}$ are unknown coefficient vectors.

In order to guarantee uniqueness on the achieved interpolation, the following equation must be satisfied

$$\mathbf{p}(\mathbf{y}) \cdot \mathbf{c}^{(i)}(\mathbf{y}) = 0 \tag{21}$$

The coefficients in Eq. 20 are determined by enforcing the interpolation pass through all n scattered nodal points within the influence domain. Thus, one can write

$$\begin{bmatrix} \tilde{\mathbf{B}} & \tilde{\mathbf{P}} \\ \tilde{\mathbf{P}}^T & \tilde{\mathbf{0}} \end{bmatrix} \cdot \begin{Bmatrix} \mathbf{c} \\ \mathbf{a} \end{Bmatrix} = \begin{Bmatrix} \mathbf{u} \\ \mathbf{0} \end{Bmatrix} \Longleftrightarrow \tilde{\mathbf{G}} \cdot \begin{Bmatrix} \mathbf{c} \\ \mathbf{a} \end{Bmatrix} = \begin{Bmatrix} \mathbf{u} \\ \mathbf{0} \end{Bmatrix} \tag{22}$$

where $\mathbf{u} = \left\{\mathbf{u}^{(1)} \ldots \mathbf{u}^{(n)}\right\}^T$ is a vector comprising the displacement vectors corresponding to the nodal points belonging in the influence domain of point $\mathbf{y}$, while the matrices $\tilde{\mathbf{B}}$ and $\tilde{\mathbf{P}}$ have the form

$$\tilde{\mathbf{B}} = \begin{bmatrix} b_1(\mathbf{x}^{(1)}) & b_2(\mathbf{x}^{(1)}) & \ldots & b_n(\mathbf{x}^{(1)}) \\ b_1(\mathbf{x}^{(2)}) & b_2(\mathbf{x}^{(2)}) & \ldots & b_n(\mathbf{x}^{(2)}) \\ \vdots & \vdots & & \vdots \\ b_1(\mathbf{x}^{(n)}) & b_2(\mathbf{x}^{(n)}) & \ldots & b_n(\mathbf{x}^{(n)}) \end{bmatrix} \tag{23}$$

$$\tilde{\mathbf{P}} = \begin{bmatrix} \mathbf{p}(\mathbf{x}^{(1)}) & \ldots & \mathbf{p}(\mathbf{x}^{(n)}) \end{bmatrix} \tag{24}$$

In the present work, the following Multiquadrics radial basis function is chosen

$$b_i(\mathbf{x}^{(j)}) = \left(d_i^2 + R^2\right)^q \tag{25}$$

where $q = 0.5$, d_i is the Euclidean distance between points $\mathbf{x}^{(i)}$ and $\mathbf{x}^{(j)}$, and R is a shape parameter equal to the minimum distance of the pairs of nodes: $(\mathbf{y}, \mathbf{x}^{(1)}), \ldots, (\mathbf{y}, \mathbf{x}^{(n)})$.

Determining $\mathbf{a}^{(i)}$ and $\mathbf{c}^{(i)}$ via Eq. 22 and considering the Multiquadrics radial basis function of Eq. 25, the interpolation scheme represented by Eq. 20 is written as

$$u_i(\mathbf{y}) = \left\{\mathbf{b}^T(\mathbf{y}) \quad \mathbf{p}^T(\mathbf{y})\right\} \cdot \tilde{\mathbf{G}}^{-1}\left(\mathbf{y}, \mathbf{x}^{(j)}\right) \cdot \begin{Bmatrix} \mathbf{u}^{(i)} \\ \mathbf{0} \end{Bmatrix} \tag{26}$$

or in vector form

$$\mathbf{u}(\mathbf{y}) = \sum_{j=1}^{n} \phi\left(\mathbf{y}, \mathbf{x}^{(j)}\right) \mathbf{u}\left(\mathbf{x}^{(j)}\right) \tag{27}$$

where the shape functions are defined by

$$\phi\left(\mathbf{y}, \mathbf{x}^{(j)}\right) = \sum_{k=1}^{n} b_k(\mathbf{y}) G_{kj}^{-1}\left(\mathbf{y}, \mathbf{x}^{(k)}\right) + \sum_{l=1}^{n} p_l(\mathbf{y}) G_{(n+l)j}^{-1}\left(\mathbf{y}, \mathbf{x}^{(l)}\right) \tag{28}$$

The derivatives of shape functions are easily obtained as

$$\phi_{,y}\left(\mathbf{y},\mathbf{x}^{(j)}\right)=\sum_{k=1}^{n}b_{k,y}\left(\mathbf{y}\right)G_{kj}^{-1}\left(\mathbf{y},\mathbf{x}^{(k)}\right)+\sum_{l=1}^{n}p_{l,y}\left(\mathbf{y}\right)G_{(n+l)j}^{-1}\left(\mathbf{y},\mathbf{x}^{(l)}\right) \tag{29}$$

As soon as the derivatives of shape functions are determined, the representation of tractions via the RBPIF is accomplished either by Eq. 15 or by Eq. 19.

3 LBIE formulations

In this section, five different MLPG(LBIE) formulations are presented. As it is already mentioned, the main differences of these formulations are concentrated on the treatment of traction vectors on the local and global boundaries involved in the LBIEs of a typical MLPG(LBIE) formulation. Thus, the departure point will be the presentation of the LBIEs used in the aforementioned MLPG(LBIE) methods.

Consider a two-dimensional linear elastic continuum domain Ω with boundary Γ, where body forces are assumed to be negligible. The displacement field $\mathbf{u}$ at any point of the domain satisfies the Navier-Cauchy equation of equilibrium

$$\mu\nabla_{\mathbf{x}}^{2}\mathbf{u}\left(\mathbf{x}\right)+\left(\lambda+\mu\right)\nabla_{\mathbf{x}}\nabla_{\mathbf{x}}\cdot\mathbf{u}\left(\mathbf{x}\right)=\mathbf{0} \tag{30}$$

with $\nabla_{\mathbf{x}}$ being the gradient operator.

The Boundary Conditions (BCs) are assumed to be

$$\begin{aligned}\mathbf{u}\left(\mathbf{x}\right)&=\mathbf{U}\left(\mathbf{x}\right),\mathbf{x}\in\Gamma_{u}\\ \mathbf{t}\left(\mathbf{x}\right)&=\mathbf{T}\left(\mathbf{x}\right),\mathbf{x}\in\Gamma_{t}\end{aligned} \tag{31}$$

where $\mathbf{U}$, $\mathbf{T}$ represent the prescribed displacement and traction vectors on the boundary sections Γ_u and Γ_t ($\Gamma_u\cup\Gamma_t\equiv\Gamma$), respectively.

The integral representation of the above described problem for an arbitrary chosen nodal point $\mathbf{x}^{(k)}$ is [Polyzos, Tsinopoulos, and Beskos (1998)]

$$a\,\mathbf{u}\left(\mathbf{x}^{(k)}\right)+\int_{\Gamma}\tilde{\mathbf{t}}^{*}\left(\mathbf{x}^{(k)},\mathbf{y}\right)\cdot\mathbf{u}\left(\mathbf{y}\right)dS_{\mathbf{y}}=\int_{\Gamma}\tilde{\mathbf{u}}^{*}\left(\mathbf{x}^{(k)},\mathbf{y}\right)\cdot\mathbf{t}\left(\mathbf{y}\right)dS_{\mathbf{y}} \tag{32}$$

where $\tilde{\mathbf{u}}^{*}$, $\tilde{\mathbf{t}}^{*}$ are the two-dimensional static fundamental displacement and traction solution kernels, respectively.

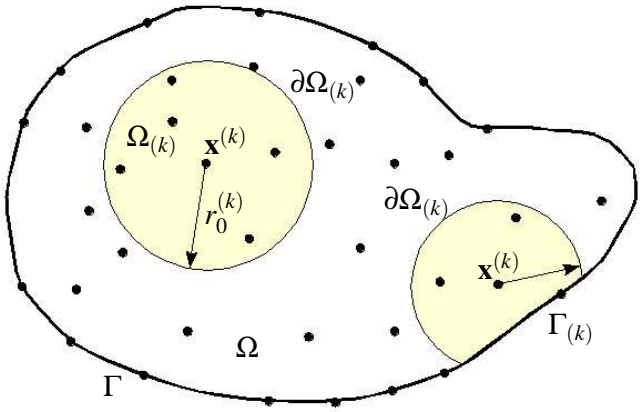

Figure 2 : Local domains $\Omega_{(k)}$ for arbitrary nodes $\mathbf{x}^{(k)}$ with support domain radius $r_0^{(k)}$, inside the domain Ω with global boundary Γ.

and

$$a=\begin{cases}1/2,\ \mathbf{x}^{(k)}\in\Gamma\\ 1,\ \mathbf{x}^{(k)}\in\Omega\\ 0,\ \mathbf{x}^{(k)}\notin\Omega\cup\Gamma\end{cases} \tag{33}$$

Since both $\tilde{\mathbf{u}}^{*}$ and $\tilde{\mathbf{t}}^{*}$ become singular only when the field point $\mathbf{y}$ approaches the source point $\mathbf{x}^{(k)}$, Eq. 32 can also be written in the form

$$a\,\mathbf{u}\left(\mathbf{x}^{(k)}\right)+\int_{\partial\Omega_{(k)}\cup\Gamma_{(k)}}\tilde{\mathbf{t}}^{*}\left(\mathbf{x}^{(k)},\mathbf{y}\right)\cdot\mathbf{u}\left(\mathbf{y}\right)dS_{\mathbf{y}}=\int_{\partial\Omega_{(k)}\cup\Gamma_{(k)}}\tilde{\mathbf{u}}^{*}\left(\mathbf{x}^{(k)},\mathbf{y}\right)\cdot\mathbf{t}\left(\mathbf{y}\right)dS_{\mathbf{y}} \tag{34}$$

where $\partial\Omega_{(k)}$ is the boundary of the support domain $\Omega_{(k)}$ corresponding to point $\mathbf{x}^{(k)}$ and defined in section 2, while $\Gamma_{(k)}$ is the part of Γ intersected by $\Omega_{(k)}$, as shown in Fig. 2. In the case where the support domain of the source point does not intersect the global boundary then the boundary integrals on $\Gamma_{(k)}$ vanish.

Eq. 34 can be further simplified into a new form by removing the boundary integral over $\partial\Omega_{(k)}$ containing the unknown traction vectors $\mathbf{t}$. According to [Atluri and Zhu (2000)] this can be accomplished with the aid of a companion solution $\tilde{\mathbf{u}}^{c}$, which satisfies the following boundary value problem:

$$\begin{aligned}&\mu\nabla_{\mathbf{y}}^{2}\tilde{\mathbf{u}}^{c}\left(\mathbf{x}^{(k)},\mathbf{y}\right)+\left(\lambda+\mu\right)\nabla_{\mathbf{y}}\nabla_{\mathbf{y}}\cdot\tilde{\mathbf{u}}^{c}\left(\mathbf{x}^{(k)},\mathbf{y}\right)=\mathbf{0},\quad\mathbf{y}\in\Omega_{(k)}\\ &\tilde{\mathbf{u}}^{c}\left(\mathbf{x}^{(k)},\mathbf{y}\right)=\tilde{\mathbf{u}}^{*}\left(\mathbf{x}^{(k)},\mathbf{y}\right),\ \mathbf{y}\in\partial\Omega_{(k)}\end{aligned} \tag{35}$$

Making use of $\tilde{\mathbf{u}}^c$, Eq. 34 can be transformed to [Sellountos and Polyzos (2005b)]

$$a\,\mathbf{u}\left(\mathbf{x}^{(k)}\right)+\int_{\partial\Omega_{(k)}\cup\Gamma_{(k)}}\tilde{\mathbf{t}}^{**}\left(\mathbf{x}^{(k)},\mathbf{y}\right)\cdot\mathbf{u}\left(\mathbf{y}\right)dS_{\mathbf{y}}=\int_{\Gamma_{(k)}}\tilde{\mathbf{u}}^{**}\left(\mathbf{x}^{(k)},\mathbf{y}\right)\cdot\mathbf{t}\left(\mathbf{y}\right)dS_{\mathbf{y}}\tag{36}$$

where $\tilde{\mathbf{u}}^{**}=\tilde{\mathbf{u}}^{*}-\tilde{\mathbf{u}}^{c}$ and $\tilde{\mathbf{t}}^{**}=\tilde{\mathbf{t}}^{*}-\tilde{\mathbf{t}}^{c}$.

3.1 MLPG(LBIE) formulation 1

Considering the LBIE of Eq. 36 and expanding both $\mathbf{u}$ and $\mathbf{t}$ according to Eq. 11 and Eq. 19, respectively, one obtains

$$\begin{aligned}&a\sum_{j}\phi\left(\mathbf{x}^{(k)},\mathbf{x}^{(j)}\right)\overline{\mathbf{u}}\left(\mathbf{x}^{(j)}\right)\\&+\sum_{j}\int_{\partial\Omega_{(k)}\cup\Gamma_{(k)}}\tilde{\mathbf{t}}^{**}\left(\mathbf{x}^{(k)},\mathbf{y}\right)\phi\left(\mathbf{y},\mathbf{x}^{(j)}\right)dS_{\mathbf{y}}\cdot\overline{\mathbf{u}}\left(\mathbf{x}^{(j)}\right)\\&=\sum_{j}\int_{\Gamma_{(k)}}\tilde{\mathbf{u}}^{**}\left(\mathbf{x}^{(k)},\mathbf{y}\right)\phi\left(\mathbf{y},\mathbf{x}^{(j)}\right)dS_{\mathbf{y}}\cdot\overline{\mathbf{t}}\left(\mathbf{x}^{(j)}\right)\end{aligned}\tag{37}$$

with $\overline{\mathbf{u}}$, $\overline{\mathbf{t}}$ being either the fictitious nodal displacements and traction values $\hat{\mathbf{u}}$ and $\hat{\mathbf{t}}$, respectively, when the MLS approximation scheme is used, or the true nodal ones $\mathbf{u}$ and $\mathbf{t}$, when the RBPIF are employed.

Collocating Eq. 37 at all nodes of the discretized model, a set of linear algebraic equations is derived, written in matrix form as

$$\tilde{\mathbf{H}}\cdot\overline{\mathbf{u}}=\tilde{\mathbf{G}}\cdot\overline{\mathbf{t}}\tag{38}$$

where the martices $\tilde{\mathbf{H}}$ and $\tilde{\mathbf{G}}$ contain non-singular, weakly singular and strongly singular integrals, the form and the numerical evaluation of which are explained in detail in the work of [Sellountos and Polyzos (2003)].

The BCs are applied straighforward on Eq. 38. For the case of the MLS approximation, this is possible only when a relatively uniform mesh is met [Li and Liu (2002); Sellountos and Polyzos (2003)]. However, for the sake of comparison both uniform and non-uniform distribution of points are utilized in the present MLPG(LBIE)/MLS formulation. Separating known from unknown nodal quantities, one concludes to a final linear system of equations

$$\tilde{\mathbf{A}}\cdot\mathbf{v}=\mathbf{b}\tag{39}$$

where the vectors $\mathbf{v}$ and $\mathbf{b}$ contain the unknown and known, respectively, nodal displacements and/or tractions, while matrix $\tilde{\mathbf{A}}$ is sparse, reflecting thus the local nature of the MLPG(LBIE) methodology.

3.2 MLPG(LBIE) formulation 2

It is well known that MLS scheme does not interpolate data. Consequently, in order to satisfy the essential BCs, for an arbitrary type of node distribution, a very simple linear transformation has been proposed [Atluri, Kim, and Cho (1999)]:

$$\mathbf{u}\left(\mathbf{y}\right)=\sum_{j=1}^{n}\varphi\left(\mathbf{y},\mathbf{x}^{(j)}\right)\mathbf{u}\left(\mathbf{x}^{(j)}\right)\tag{40}$$

where

$$\varphi\left(\mathbf{y},\mathbf{x}^{(j)}\right)=\sum_{i=1}^{n}\frac{\phi\left(\mathbf{y},\mathbf{x}^{(j)}\right)}{\phi\left(\mathbf{x}^{(j)},\mathbf{x}^{(i)}\right)}\tag{41}$$

Obviously, this tranformation is not valid if the RBPIF scheme is used.

Adopting the interpolation scheme of Eq. 40 instead that of Eq. 11 for both displacements ad tractions, Eq. 36 obtains the form

$$\begin{aligned}&a\sum_{j}\varphi\left(\mathbf{x}^{(k)},\mathbf{x}^{(j)}\right)\mathbf{u}\left(\mathbf{x}^{(j)}\right)\\&+\sum_{j}\int_{\partial\Omega_{(k)}\cup\Gamma_{(k)}}\tilde{\mathbf{t}}^{**}\left(\mathbf{x}^{(k)},\mathbf{y}\right)\cdot\varphi\left(\mathbf{y},\mathbf{x}^{(j)}\right)dS_{\mathbf{y}}\cdot\mathbf{u}\left(\mathbf{x}^{(j)}\right)\\&=\sum_{j}\int_{\Gamma_{(k)}}\tilde{\mathbf{u}}^{**}\left(\mathbf{x}^{(k)},\mathbf{y}\right)\varphi\left(\mathbf{y},\mathbf{x}^{(j)}\right)dS_{\mathbf{y}}\cdot\mathbf{t}\left(\mathbf{x}^{(j)}\right)\end{aligned}\tag{42}$$

Collocating at all nodes of the discretized model, a system similar to that of Eq. 38 is obtained with vectors $\overline{\mathbf{u}}$, $\overline{\mathbf{t}}$ representing the exact nodal values and not the fictitious ones. As a result, the BCs can be inserted directly in Eq. 38 and the final system of Eq. 39 is easily obtained.

3.3 MLPG(LBIE) formulation 3

Splitting the integrals of Eq. 36, defined on the global boundary $\Gamma_{(k)}$ ($\equiv\Gamma_{(k)u}\cup\Gamma_{(k)t}$), according to the BCs and inserting the prescribed displacement and traction values

in the integrals, it is derived that

$$
\begin{aligned}
&a\,\mathbf{u}\left(\mathbf{x}^{(k)}\right)+\int_{\partial\Omega_{(k)}\cup\Gamma_{(k)t}}\tilde{\mathbf{t}}^{**}\left(\mathbf{x}^{(k)},\mathbf{y}\right)\cdot\mathbf{u}\left(\mathbf{y}\right)dS_{\mathbf{y}}\\
&\quad+\int_{\Gamma_{(k)u}}\tilde{\mathbf{t}}^{**}\left(\mathbf{x}^{(k)},\mathbf{y}\right)\cdot\mathbf{U}\left(\mathbf{y}\right)dS_{\mathbf{y}}\\
&\quad=\int_{\Gamma_{(k)u}}\tilde{\mathbf{u}}^{**}\left(\mathbf{x}^{(k)},\mathbf{y}\right)\cdot\mathbf{t}\left(\mathbf{y}\right)dS_{\mathbf{y}}\\
&\quad+\int_{\Gamma_{(k)t}}\tilde{\mathbf{u}}^{**}\left(\mathbf{x}^{(k)},\mathbf{y}\right)\cdot\mathbf{T}\left(\mathbf{y}\right)dS_{\mathbf{y}}
\end{aligned}
\tag{43}
$$

Making use of Eq. 11 and Eq. 15, wherever there are unknown displacement and traction vectors, Eq. 43 yields

$$
\begin{aligned}
&a\left\langle\begin{array}{c}\sum_j\phi\left(\mathbf{x}^{(k)},\mathbf{x}^{(j)}\right)\overline{\mathbf{u}}\left(\mathbf{x}^{(j)}\right)\\ \text{or}\\ \mathbf{U}\left(\mathbf{x}^{(k)}\right)\end{array}\right\rangle\\
&\quad+\sum_j\int_{\partial\Omega_{(k)}\cup\Gamma_{(k)t}}\tilde{\mathbf{t}}^{**}\left(\mathbf{x}^{(k)},\mathbf{y}\right)\phi\left(\mathbf{y},\mathbf{x}^{(j)}\right)dS_{\mathbf{y}}\cdot\overline{\mathbf{u}}\left(\mathbf{x}^{(j)}\right)\\
&\quad+\int_{\Gamma_{(k)u}}\tilde{\mathbf{t}}^{**}\left(\mathbf{x}^{(k)},\mathbf{y}\right)\cdot\mathbf{U}\left(\mathbf{y}\right)dS_{\mathbf{y}}\\
&\quad=\sum_j\int_{\Gamma_{(k)u}}\tilde{\mathbf{u}}^{**}\left(\mathbf{x}^{(k)},\mathbf{y}\right)\cdot\tilde{\mathbf{N}}\left(\mathbf{y}\right)\cdot\tilde{\mathbf{D}}\cdot\tilde{\mathbf{E}}\left(\mathbf{y},\mathbf{x}^{(j)}\right)dS_{\mathbf{y}}\\
&\quad\cdot\overline{\mathbf{u}}\left(\mathbf{x}^{(j)}\right)+\int_{\Gamma_{(k)t}}\tilde{\mathbf{u}}^{**}\left(\mathbf{x}^{(k)},\mathbf{y}\right)\cdot\mathbf{T}\left(\mathbf{y}\right)dS_{\mathbf{y}}
\end{aligned}
\tag{44}
$$

where $\overline{\mathbf{u}}$ represents the fictitious nodal displacements when the MLS approximation scheme is used, or the exact ones in the case of the RBPIF.

It should be noted here that Eq. 44 contains derivatives of shape functions only when the support domain of point $\mathbf{x}^{(k)}$ intersects the global boundary Γ in a part where the displacement vector is prescribed ($\Gamma_{(k)u}$). Perfoming all the numerical integrations, as in the previous formulations, a final system of linear algebraic equations similar to that of Eq. 39, is obtained.

Depending on the type of interpolation functions, the solution of this system provides all the fictitious or exact displacement values of the considered elastic problem.

3.4 MLPG(LBIE) formulation 4

In this formulation, Eq. 34 instead of Eq. 36 is employed. On the global boundary both displacements and tractions are treated as independet variables, while the tractions defined on the local boundaries $\partial\Omega_{(k)}$ are analyzed via the representation of Eq. 15. Thus, one can write

$$
\begin{aligned}
&a\sum_j\phi\left(\mathbf{x}^{(k)},\mathbf{x}^{(j)}\right)\overline{\mathbf{u}}\left(\mathbf{x}^{(j)}\right)\\
&\quad+\sum_j\int_{\partial\Omega_{(k)}\cup\Gamma_{(k)}}\tilde{\mathbf{t}}^{*}\left(\mathbf{x}^{(k)},\mathbf{y}\right)\phi\left(\mathbf{y},\mathbf{x}^{(j)}\right)dS_{\mathbf{y}}\cdot\overline{\mathbf{u}}\left(\mathbf{x}^{(j)}\right)\\
&\quad=\sum_j\int_{\partial\Omega_{(k)}}\tilde{\mathbf{u}}^{*}\left(\mathbf{x}^{(k)},\mathbf{y}\right)\cdot\tilde{\mathbf{N}}\left(\mathbf{y}\right)\cdot\tilde{\mathbf{D}}\cdot\tilde{\mathbf{E}}\left(\mathbf{y},\mathbf{x}^{(j)}\right)dS_{\mathbf{y}}\\
&\quad\cdot\overline{\mathbf{u}}\left(\mathbf{x}^{(j)}\right)+\sum_j\int_{\Gamma_{(k)}}\tilde{\mathbf{u}}^{*}\left(\mathbf{x}^{(k)},\mathbf{y}\right)\phi\left(\mathbf{y},\mathbf{x}^{(j)}\right)dS_{\mathbf{y}}\cdot\overline{\mathbf{t}}\left(\mathbf{x}^{(j)}\right)
\end{aligned}
\tag{45}
$$

Collocating Eq. 45 at all nodes of the discretized model, a set of linear equations similar to that of Eq. 38 is formed and the solution procedure is exactly the same as that described in the first formulation.

3.5 MLPG(LBIE) formulation 5

This formulation, as the previous one, utilizes Eq. 34 and for the treatment of BCs exploits the procedure adopted in the third formulation. Thus, Eq. 34 for the k-th node is the one below

$$
\begin{aligned}
&a\left\langle\begin{array}{c}\sum_j\phi\left(\mathbf{x}^{(k)},\mathbf{x}^{(j)}\right)\overline{\mathbf{u}}\left(\mathbf{x}^{(j)}\right)\\ \text{or}\\ \mathbf{U}\left(\mathbf{x}^{(k)}\right)\end{array}\right\rangle\\
&\quad+\sum_j\int_{\partial\Omega_{(k)}\cup\Gamma_{(k)t}}\tilde{\mathbf{t}}^{*}\left(\mathbf{x}^{(k)},\mathbf{y}\right)\phi\left(\mathbf{y},\mathbf{x}^{(j)}\right)dS_{\mathbf{y}}\cdot\overline{\mathbf{u}}\left(\mathbf{x}^{(j)}\right)\\
&\quad+\int_{\Gamma_{(k)u}}\tilde{\mathbf{t}}^{*}\left(\mathbf{x}^{(k)},\mathbf{y}\right)\cdot\mathbf{U}\left(\mathbf{y}\right)dS_{\mathbf{y}}\\
&\quad=\sum_j\int_{\partial\Omega_{(k)}\cup\Gamma_{(k)u}}\tilde{\mathbf{u}}^{*}\left(\mathbf{x}^{(k)},\mathbf{y}\right)\cdot\tilde{\mathbf{N}}\left(\mathbf{y}\right)\cdot\tilde{\mathbf{D}}\cdot\tilde{\mathbf{E}}\left(\mathbf{y},\mathbf{x}^{(j)}\right)dS_{\mathbf{y}}\\
&\quad\cdot\overline{\mathbf{u}}\left(\mathbf{x}^{(j)}\right)+\int_{\Gamma_{(k)t}}\tilde{\mathbf{u}}^{*}\left(\mathbf{x}^{(k)},\mathbf{y}\right)\cdot\mathbf{T}\left(\mathbf{y}\right)dS_{\mathbf{y}}
\end{aligned}
\tag{46}
$$

Collocating Eq. 46 at all nodes and following the solution procedure of the previous formulation the unknown nodal displacements are evaluated. Comparing with MLPG(LBIE) formulation 4, one can say that the present formulation employs LBIEs comprising derivatives of the MLS or RBPIF shape functions for all considered nodal points.

4 Numerical Examples

In this section two elastostatic problems, known in the literature as Lamé and Kirsch problems, are solved with

the aid of the five MLPG formulations presented in the previous section. For comparison purposes of the present work, the displacement relative error L_2 norm in logarithmic scale, i.e.

$$err_u = log_{10}\sqrt{\frac{\|\mathbf{u}^{analytical} - \mathbf{u}^{numerical}\|^2}{\|\mathbf{u}^{analytical}\|^2}} \tag{47}$$

is evaluated for both problems and for the five MLPG(LBIE) formulations.

4.1 Lamé problem

Consider a cylinder of unit external radius and thickness equal to $0.2cm$, as shown in Fig. 3, subjected to internal pressure load of magnitude equal to $10Pa$. Due to symmetry of the problem only one quadrant is analyzed with 130 uniformly distributed nodes covering both the interior and the boundary of the cylinder (Fig. 4). Since the mesh is uniform, all nodes are set in the numerical calculations to share the same support domain radius. The material properties are considered to be $E = 4.22kPa$ for Young modulus of elasticity and $\nu = 0.25$ for Poisson ratio. The exact solution of the Lamé problem can be found in the book of [Timoshenko and Goodier (1970)].

Fig. 5 depicts the displacement relative error L_2 norm, evaluated for the five MLPG(LBIE) formulations, as a function of the dimensionless ratio of the support domain radius r_0 of all nodes to the Euclidean distance d of two close-distant nodes. The same error measures are displayed in Fig. 6, where the RBPIF scheme is exploited.

For a uniform distribution of points Fig. 5 and Fig. 6 show that:

- MLS approximation scheme provides more accurate results than the RBPIF one. It should be noted, however, that this remark is valid for the weighted functions and constant considered in the MLS and RBPIF schemes, explained in subsections 2.1 and 2.2. No parametric study on the determination of the optimum shape parameters of the utilized interpolation schemes is carried out in the context of the present work.

- Higher accuracy is accomplished with the aid of formulation 1 and 3. Furthermoe, when the MLS approximation scheme is employed, formulation 1 increases its accuracy as the support domain of each nodal point increases, while formulation 3 seems to be independed of the size of the considered support domains.

- The use of derivatives of the MLS and RBPIF shape functions on the local boundary of the support domains, affects drastically the solution accuracy and the stability of a MLPG(LBIE) formulation.

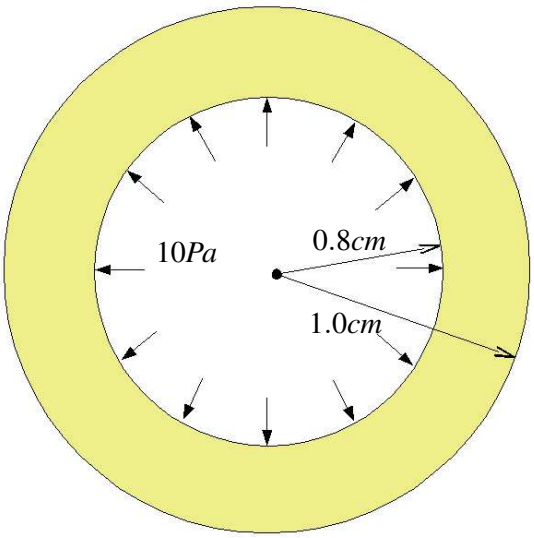

Figure 3 : Lamé's problem of a cylinder subjected to a uniform internal pressure load.

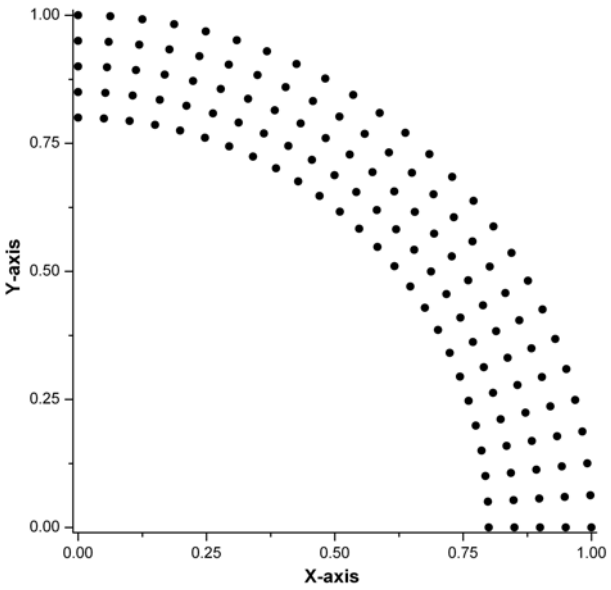

Figure 4 : Cylinder quadrant discretized with uniformly distributed nodes.

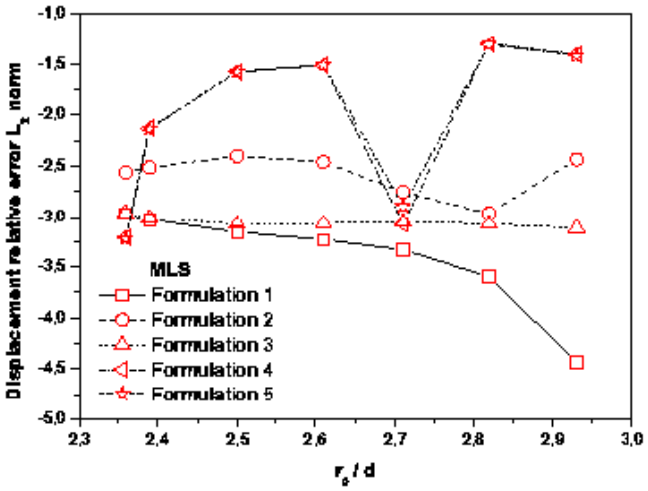

Figure 5 : Displacement relative error L_2 norm for various support domain radii when the MLS scheme is used, for the Lamé problem.

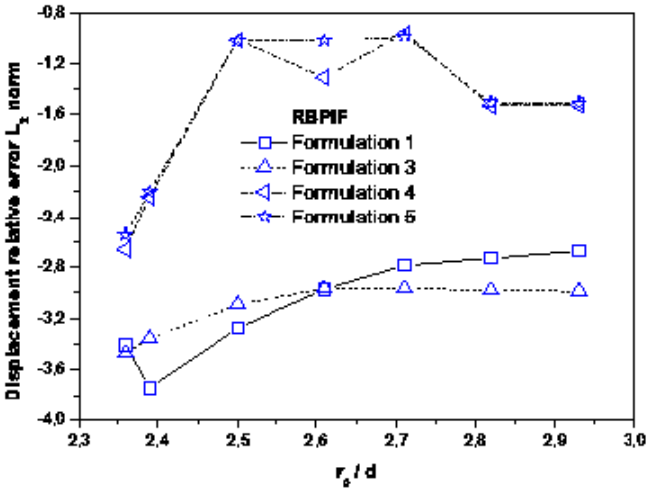

Figure 6 : Displacement relative error L_2 norm for various support domain radii when the RBPIF scheme is used, for the Lamé problem.

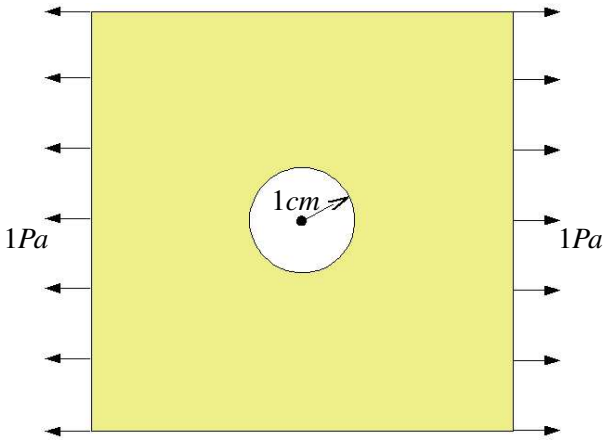

Figure 7 : Kirsch's problem of the infinite plate subjected to a uniform tensile load.

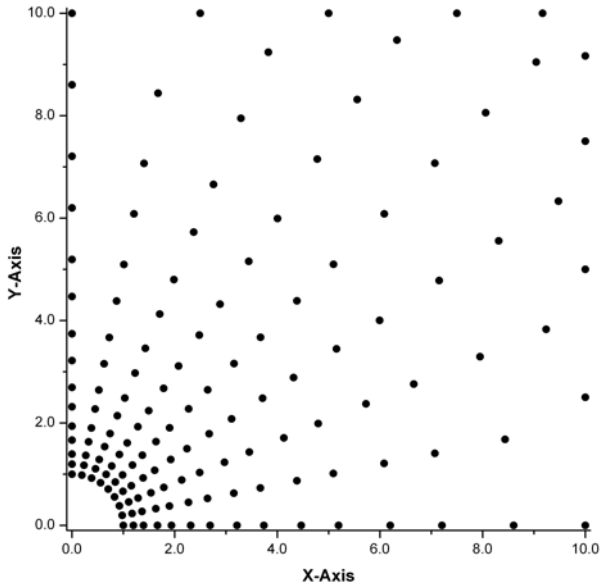

Figure 8 : Distribution of nodes on the quarter part of the plate with hole.

4.2 Kirsch problem

The Kirsch problem is that shown in Fig. 7 where a plate with a circular hole, located in the center, subjected to plane stress. For symmetry reasons only the upper right $10cm \times 10cm$ quadrant is analyzed, as shown in Fig. 8, while the hole has $1cm$ radius. 145 non-uniform nodes are used to discretize the model, with the node distribution being more dense near to the central hole of the plate. Due to the pattern of point distribution, the nodes that have the same radial distance from the center of the plate have the same support domain radius. In order to keep the ratio r_0/d constant for each nodal point, the support domain radius r_0 increases as the radial distance at the points increases. Of course the criterion of adequate support domain overlapping is fulfilled. The material properties are considered to be: $E = 4.2kPa$ and $\nu = 0.25$. The analytical solutions for this problem can be found in [Timoshenko and Goodier (1970)].

Fig. 9 and Fig. 10 depict the displacement relative er-

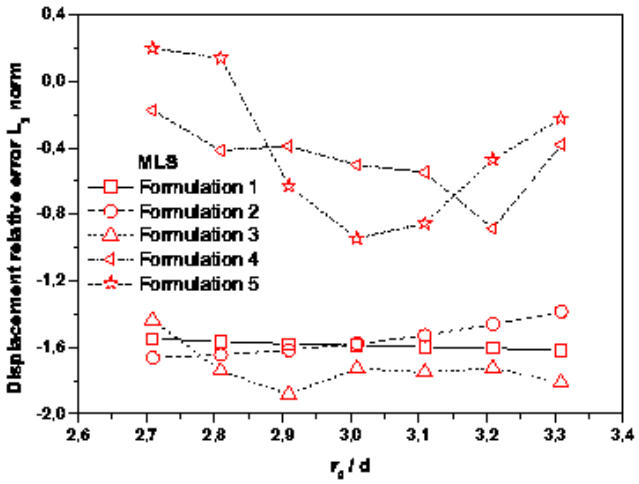

Figure 9 : Displacement relative error L_2 norm for various support domain radii when the MLS scheme is used, for the Kirsch problem.

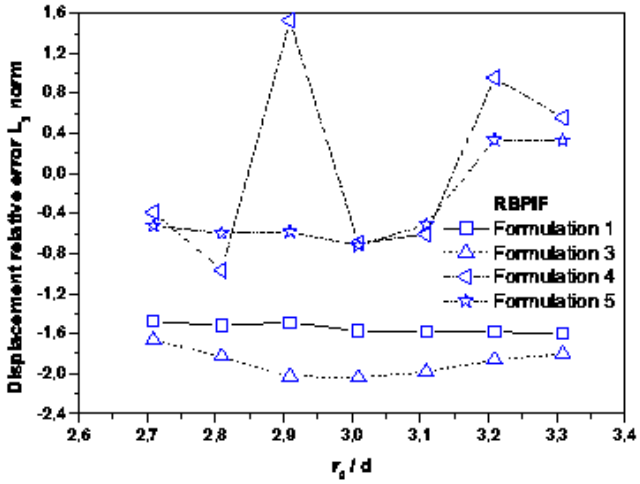

Figure 10 : Displacement relative error L_2 norm for various support domain radii when the RBPIF scheme is used, for the Kirsch problem.

ror L_2 norm in depedence to the dimensionless mean ratio of the support domain radius to the minimum distance of two neighborhood nodes for both approximation/interpolation schemes, respectively.

In view of Fig. 9 and Fig. 10, the following remarks have to be made:

- For non-uniform distribution of points, both MLPG(LBIE)/MLS and MLPG(LBIE)/RBPIF formulations provide comparable results.
- Higher accuracy and stability is accomplished via formulations 1, 2 and 3.
- As in the previous numerical example, the use of derivatives of shape functions in the integrals defined on the local boundaries affects the accuracy and the stability of the studied MLPG(LBIE) formulations.

5 Conclusions

A comparison study on five MLPG(LBIE) formulations has been made in the present work. Both MLS approximation and RBPIF schemes are used in their implementation. In brief the main characteristics of these five formulations are:

MLPG(LBIE) formulation 1: It is identical to that proposed by [Sellountos and Polyzos (2003)]. No shape function derivatives are involved in this formulation, since the companion solution is exploited and on the global boundary displacements and tractions are interpolated as independet variables. When the MLS approximation scheme is utilized, the BCs are imposed directly on the fictitious $\hat{u}$ and $\hat{t}$.

MLPG(LBIE) formulation 2: This formulation is the same with the previous one, utilizing however the inverse MLS approximation scheme of [Atluri, Kim, and Cho (1999)] where the exact nodal displacement vectors and not the fictitious ones are involved in the MLS shape functions.

MLPG(LBIE) formulation 3: The main difference of this formulation, as it is compared to the previous ones, is that it treats the unknown global boundary traction vector through Hooke's law, inserting thus derivatives of shape functions in LBIEs valid for some nodal points lying on the global boundary of the analyzed problem.

MLPG(LBIE) formulation 4: In this formulation displacements and tractions defined on the global boundary are treated in the same way as in formulation 1. On the local boundaries, however, tractions are expressed in terms of displacements inserting thus derivatives of shape functions for all the internal points.

MLPG(LBIE) formulation 5: Except the nodal points where the traction vectors are prescribed, in this formulation all traction fields are expressed through Hooke's law. Thus, derivatives of shape functions appear in LBIEs defined on internal and boundary points.

Two problems have been solved via the aforementioned MLPG(LBIE) formulations using uniform and non-uniform distribution of points. In view of the obtained results the following conclusions can be drawn:

(i) MLPG(LBIE) formulations with uniform distribution of points provide the best results. This conclusion is in agreement with the comments refered in the work of [Augarde and Deeks (2005)].

(ii) Utilizing the same constants and weighted functions in all formulations, MLPG(LBIE)/MLS solutions are more accurate than the MLPG(LBIE)/RBPIF ones.

(iii) The MLPG(LBIE) formulation 1 delivers the most accurate results even for irregularly distributed points.

(iv) The use of derivatives on the local boundary of the support domains decreases the solution accuracy of the MLPG(LBIE) formulation.

(v) Although the MLPG(LBIE) formulation 3 contains shape function derivatives in the LBIEs of some nodal points lying on the global boundary, it exhibits accuracy being comparable to that of formulation 1.

(vi) The results provided by formulations 4 and 5 show that their solution accuracy is strongly depended on the size of the support domains.

Acknowledgement: The authors would like to thank the Greek Secretariat of Research and Technology and ENVIROCOUSTICS SA for the support at this work, in the framework of the PENED-2001 research program.

References

Atluri, S. N. (2004): *The Meshless Method (MLPG) for Domain & BIE Discretization*. Tech. Science Press.

Atluri, S. N.; Han, Z. D.; Shen, S. (2003): Meshless local Petrov-Galerkin (MLPG) approaches for solving the weakly-singular traction and displacement boundary integral equations . *CMES: Computer Modeling in Engineering & Sciences*, vol. 4, pp. 507–517.

Atluri, S. N.; Kim, H.-G.; Cho, J. Y. (1999): A critical assessment of the truly Meshless Local Petrov-Galerkin (MLPG) and Local Boundary Integral Equation (LBIE) methods. *Computational Mechanics*, vol. 24, pp. 348–372.

Atluri, S. N.; Shen, S. (2002a): The meshless local Petrov-Galerkin (MLPG) method: A simple & less-costly alternative to the finite and boundary element method. *CMES: Computer Modeling in Engineering & Sciences*, vol. 3, pp. 11–52.

Atluri, S. N.; Shen, S. (2002b): *The Meshless Local Petrov-Galerkin (MLPG) Method*. Tech. Science Press.

Atluri, S. N.; Sladek, J.; Sladek, V.; Zhu, T. (2000): The local boundary integral equation (LBIE) and its meshless implementation for linear elasticity. *Computational Mechanics*, vol. 25, pp. 180–198.

Atluri, S. N.; Zhu, T. (1998): A new meshless local Petrov-Galerkin (MLPG) approach in computation mechanics. *Computational Mechanics*, vol. 22, pp. 117–127.

Atluri, S. N.; Zhu, T. (2000): New concepts in meshless methods. *International Journal of Numerical Methods in Engineering*, vol. 47, pp. 537–556.

Augarde, C. E.; Deeks, A. J. (2005): On the effects of nodal distributions for imposition of essential boundary conditions in the MLPG meshfree method. *Communications in Numerical Methods in Engineering*, vol. 21, pp. 389–395.

Beskos, D. E. (1987): Boundary element methods in dynamic analysis. *Applied Mechanics Reviews*, vol. 40, pp. 1–23.

Beskos, D. E. (1997): Boundary element methods in dynamic analysis. Part II. *Applied Mechanics Reviews*, vol. 50, pp. 149–197.

Han, Z. D.; Atluri, S. N. (2004): Meshless local Petrov-Galerkin (MLPG) approaches for solving 3D Problems in elasto-statics. *CMES: Computer Modelling in Engineering & Sciences*, vol. 6, pp. 169–188.

Lancaster, P.; Salkauskas, K. (1981): Surfaces generated by moving least squares methods. *Mathematics of Computations*, vol. 37, pp. 141–158.

Li, S.; Liu, W. K. (2002): Meshfree and particle methods and their applications. *Applied Mechanics Reviews*, vol. 54, pp. 1–34.

Long, S.; Zhang, Q. (2002): Analysis of thin plates by the local boundary integral equation (LBIE) method. *Engineering Analysis with Boundary Elements*, vol. 26, pp. 707–718.

Polyzos, D.; Tsinopoulos, S. V.; Beskos, D. E. (1998): Static and dynamic boundary element analysis in incompressible linear elasticity. *European Journal of Mechanics, A/Solids*, vol. 17, pp. 515–536.

Qian, Z. Y.; Han, Z. D.; Atluri, S. N. (2004): Directly Derived Non-Hyper-Singular Boundary Integral Equations for Acoustic Problems, and their Solution through Petrov-Galerkin Schemes. *CMES: Computer Modelling in Engineering & Sciences*, vol. 5, no. 6, pp. 541–562.

Sellountos, E. J.; Polyzos, D. (2003): A MLPG (LBIE) method for solving frequency domain elastic problems. *CMES: Computer Modelling in Engineering & Sciences*, vol. 4, pp. 619–636.

Sellountos, E. J.; Polyzos, D. (2005a): A MLPG (LBIE) approach in combination with BEM. *Computer Methods in Applied Mechanics and Engineering*, vol. 194, pp. 859–875.

Sellountos, E. J.; Polyzos, D. (2005b): A meshless local boundary integral equation method for solving transient elastodynamic problems. *Computational Mechanics*, vol. 35, pp. 265–276.

Sellountos, E. J.; Vavourakis, V.; Polyzos, D. (2005): A new Singular/Hypersingular MLPG (LBIE) method for 2D elastostatics. *CMES: Computer Modeling in Engineering & Sciences*, vol. 7, no. 1, pp. 35–48.

Sladek, J.; Sladek, V. (2003): Application of local boundary integral method in to micropolar elasticity. *Engineering Analysis with Boundary Elements*, vol. 27, pp. 81–90.

Sladek, J.; Sladek, V.; Atluri, S. N. (2001): A pure contour formulation formulation for meshless local boundary integral equation method in thermoelasticity . *CMES: Computer Modeling in Engineering & Sciences*, vol. 2, pp. 423–434.

Sladek, J.; Sladek, V.; Atluri, S. N. (2002): Application of the local boundary integral equation method to boundary value problems. *International Journal of Applied Mechanics*, vol. 38, pp. 1025–1043.

Sladek, J.; Sladek, V.; Bazant, Z. P. (2003): Non-local boundary integral formulation for softening damage. *International Journal for Numerical Methods in Engineering*, vol. 57, pp. 103–116.

Sladek, J.; Sladek, V.; Keer, R. V. (2000): Numerical integration of singularities of local boundary integral equations. *Computational Mechanics*, vol. 25, pp. 394–403.

Sladek, J.; Sladek, V.; Krivacek, J.; Zhang, C. (2003): Local BIEM for transient heat conduction analysis in 3D axisymmetric functionally graded solids. *Computational Mechanics*, vol. 32, pp. 169–176.

Sladek, J.; Sladek, V.; Mang, H. A. (2002a): Meshless formulation for simply supported and clamped plate problems. *International Journal for Numerical Methods in Engineering*, vol. 55, pp. 359–375.

Sladek, J.; Sladek, V.; Mang, H. A. (2002b): Meshless local boundary integral equation method for plates resting on the elastic foundation. *Computer Methods in Applied Mechanics and Engineering*, vol. 191, pp. 5943–5959.

Sladek, J.; Sladek, V.; Zhang, C. (2005a): A meshless local boundary integral equation method for dynamic anti-plane shear shock crack problem in functionally graded materials . *Engineering Analysis with Boundary Elements*, vol. 29, pp. 334–342.

Sladek, J.; Sladek, V.; Zhang, C. (2005b): An advanced numerical method for computing elastodynamic fracture parameters in functionally graded materials . *Computational Materials Science*, vol. 32, pp. 523–543.

Timoshenko, S. P.; Goodier, J. N. (1970): *Theory of Elasticity*. McGraw-Hill.

Wang, J. G.; Liu, G. R. (2002): A point interpolation meshless method based on radial basis functions. *International Journal for Numerical Methods in Engineering*, vol. 54, pp. 1623–1648.

Wendland, H. (1999): Meshless Galerkin method using radial basis functions. *Mathematics of Computation*, vol. 68, pp. 1521–1531.

Zhu, T.; Zhang, J. D.; Atluri, S. N. (1998a): A local boundary integral equation (LBIE) method in computational mechanics and a meshless discretization approach. *Computational Mechanics*, vol. 21, pp. 223–235.

Zhu, T.; Zhang, J. D.; Atluri, S. N. (1998b): A meshless local boundary integral equation (LBIE) method for solving non-linear problems . *Computational Mechanics*, vol. 22, pp. 174–186.

Zhu, T.; Zhang, J. D.; Atluri, S. N. (1999): A meshless numerical method based on the local boundary integral equation (LBIE) to solve linear and non-linear boundary value problems . *Engineering Analysis with Boundary Elements*, vol. 23, pp. 375–389.